

Effects of vortex and antivortex excitations in underdoped $\text{Bi}_2\text{Sr}_2\text{Ca}_2\text{Cu}_3\text{O}_{10+\delta}$ bulk single crystals

Takao Watanabe,^{1,*} Kenta Kosugi,¹ Nae Sasaki,¹ Shunpei Yamaguchi,¹
Takenori Fujii,² Ken Hayama,³ Itsuhiro Kakeya,³ and Toshimitsu Ito⁴

¹Graduate School of Science and Technology, Hirosaki University, Hirosaki, Aomori, 036-8561 Japan

²Cryogenic Research Center, University of Tokyo, Bunkyo, Tokyo 113-0032, Japan

³Department of Electronic Science and Engineering, Kyoto University, Kyoto 615-8510, Japan

⁴Research Institute for Advanced Electronics and Photonics,

National Institute of Advanced Industrial Science and Technology (AIST), Higashi 1-1-1, Tsukuba, Ibaraki 305-8565, Japan

(Dated: October 11, 2024)

The observance of vortex and anti-vortex effects in bulk crystals can prove the existence of phase-disordered superconductivity in the bulk. To gain insights into the mechanisms that govern superconducting transition in copper oxide high-transition temperature (T_c) superconductors, this study investigated the transport properties of underdoped $\text{Bi}_2\text{Sr}_2\text{Ca}_2\text{Cu}_3\text{O}_{10+\delta}$ (Bi-2223) bulk single crystals. The I - V characteristics results and the typical tailing behavior owing to the temperature dependence of in-plane resistivity (ρ_{ab}) were consistent with the Kosterlitz-Thouless (KT) transition characteristics. Thus, with increasing temperature, copper oxide high- T_c superconductors transitioned to their normal state owing to destruction of their phase correlations, although a finite Cooper pair density was prevalent at T_c . Further, magnetization measurements were performed to determine the temperature dependence of the irreversible magnetic field B_{irr} . Consequently, the mechanism governing the KT transition-like superconducting transition in this bulk system was elucidated. These results support the extreme strong-coupling models for high- T_c superconductivity in cuprates.

I. INTRODUCTION

In conventional Bardeen, Cooper, and Schrieffer (BCS) superconductors, the amplitude of the order parameter disappears as the temperature increases till the superconducting transition temperature (T_c) is reached. However, in copper-oxide high- T_c superconductors, the order parameter phase is destroyed despite its finite amplitude, which results in a transition to a normal state [1–3]. Thus, a "phase-disordered superconductivity" is observed at temperatures higher than T_c . However, the plausibility of this theory must be investigated to elucidate the mechanism of the high- T_c superconductivity in cuprates. Despite the several interesting experimental results reported [4, 5] in previous studies, there is no consensus among researchers.

In two-dimensional (2D) superconductors, at high temperatures approaching T_c , the free vortices (circulating super-currents are counterclockwise) and anti-vortices (circulating super-currents are clockwise) are thermally excited in equal numbers. Consequently, the long-range phase ordering of superconductivity is disrupted. However, below a certain temperature (T_{KT}), vortex-anti-vortex pairs are formed individually, which undergo a phase transition to a substantial superconducting state. This is referred to as the Kosterlitz-Thouless (KT) transition [6, 7]. Therefore, the observance of vortex and anti-vortex effects in bulk crystals can prove the existence of phase-disordered superconductivity in the bulk [8].

Several studies have focused on the KT transition in cuprate high- T_c superconductors, on 1-unit-cell-thick $\text{YBa}_2\text{Cu}_3\text{O}_{7-\delta}$ (YBCO) ultra-thin films [9], 2-unit-cell Ca-doped YBCO ultrathin films [10], and 2-unit-cell $\text{Bi}_2\text{Sr}_2\text{Ca}_2\text{Cu}_3\text{O}_{10+\delta}$ (Bi-2223) that were mechanically exfoliated from the bulk crystal [11]. All these studies used 2D films. However, it is considered that the KT transition does not occur in a bulk

system with a finite interlayer coupling. This is because, it is a unique phase transition in a 2D system. Certain studies have focused on the possible KT transition; for example, $\text{La}_{1.875}\text{Ba}_{0.125}\text{CuO}_4$ bulk single crystals [12] and underdoped $\text{La}_{2-x}\text{Sr}_x\text{CuO}_4$ (LSCO) thick films (equivalent to the bulk) [13]. However, Matsuda *et al.* found [14] that even in $\text{Bi}_2\text{Sr}_2\text{CaCu}_2\text{O}_{8+\delta}$ (Bi-2212), which exhibits the strongest 2D nature among copper oxides, the occurrence of the KT transition is challenging owing to the system obeying a simple three-dimensional (3D)-XY model [15].

Multilayered high- T_c cuprates are suitable for exploring the KT transition in bulk because the inner CuO_2 planes are ideally flat and underdoped compared to the outer CuO_2 planes [16, 17]. Thus, they are expected to decouple the interplane Josephson coupling [18, 19]. Using underdoped samples of trilayered Bi-2223, for which good quality single crystals are readily available [20, 21], this study examined the possibility of the KT transition. The I - V characteristics and tailing behavior of $\rho_{ab}(T)$ indicated the occurrence of a KT transition-like superconducting transition. Furthermore, based on the measurements of the irreversible magnetic field $B_{irr}(T)$, we discussed the mechanism that enables KT transition-like vortex and anti-vortex excitations in bulk materials.

II. EXPERIMENT

High-quality Bi-2223 single crystals were grown employing the traveling solvent floating zone (TSFZ) method [21]. The raw rod composition was Bi-rich (Bi:Sr:Ca:Cu = 2.25:2:2:3), the growth atmosphere was an oxygen-argon mixture with 10 % oxygen, and the growth rate was set to 0.05 mm/h. The crystals obtained were annealed at 600 °C for 4

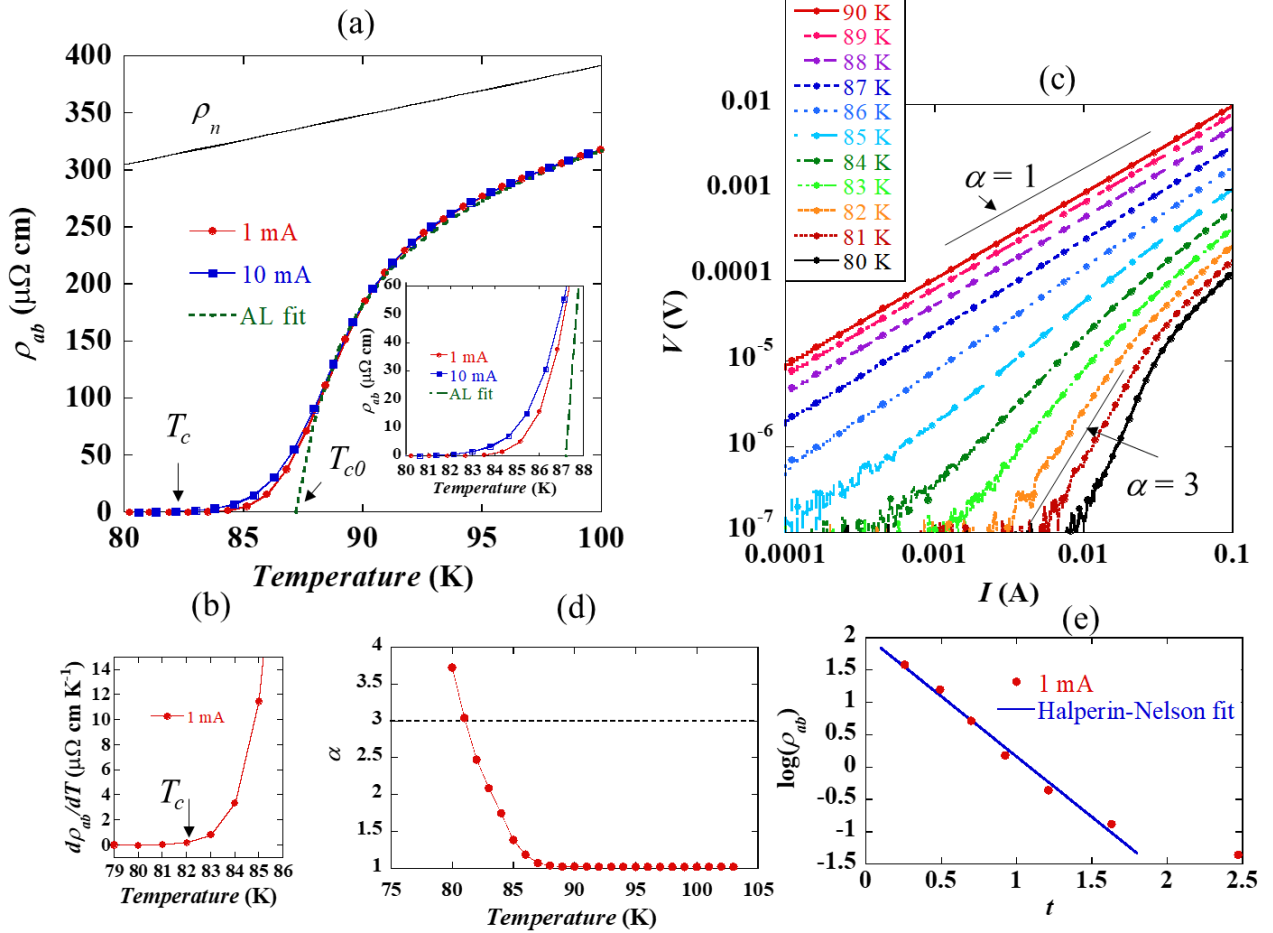


FIG. 1. (Color online) Kosterlitz-Thouless (KT)-like superconducting transition in an underdoped (UD1) Bi-2223 bulk single crystal. (a) Superconducting transition curve for a UD1 Bi-2223 single crystal. The green dashed line shows the fitting results using the 2D Aslamasov—Larkin (AL) formula for superconducting fluctuations. The mean field superconducting transition temperature (T_{c0}) is estimated to be 87 K. ρ_n is the in-plane resistivity (ρ_{ab}) in the absence of superconducting fluctuations used for the fitting, and ρ_n is assumed to be $\rho_n = aT + b$ ($a = 4.4 \mu\Omega\text{cm/K}$, $b = -55 \mu\Omega\text{cm}$). The inset shows expanded plots for non-ohmic behavior observed below 87 K. (b) The temperature dependence of $d\rho_{ab}(T)/dT$. From this, T_c is obtained as 82 K. (c) I - V characteristics at various temperatures plotted on both axes on the logarithmic scales. (d) Power exponents α found in the I - V characteristics ($V \propto I^\alpha$) as a function of temperature. α reaches a value of 3 at 81 K [the KT transition temperature (T_{KT}) = 81 K]. (e) Temperature dependence of ρ_{ab} . The straight line indicates the fitted result by the Halperin–Nelson equation, $\rho_{ab}(T) = \rho_{ab}^0 \exp(-2ct)$, where $t = [(T_{c0} - T)/(T - T_{KT})]^{1/2}$ ($\rho_{ab}^0 = 106 \mu\Omega\text{cm}$ and $c = 2.15$).

h at an oxygen partial pressure (P_{O_2}) of 5 or 2 Pa to facilitate underdoping. Hereinafter, the crystals annealed under these conditions are referred to as UD1 Bi-2223 and UD2 Bi-2223.

To obtain the I - V characteristics, pulse measurements were performed to minimize heat generation under a high current bias. A pulse period and width of 50 and 1 ms (thus, a duty ratio of 2 %), respectively, were used (Appendix A). The in-plane resistivity $\rho_{ab}(T)$ was measured using the DC 4-terminal method. Further, the magnetic susceptibility was measured using a superconducting quantum interference device magnetometer (Quantum Design Magnetic Property Measurement System). Irreversible magnetic fields (B_{irr}) were obtained through measurements of the temperature dependence of magnetic susceptibility under various magnetic

fields ($B \parallel c$) up to 7 T for both zero-field cooling (ZFC) and cooling in a magnetic field (FC). All the temperature sweep rates were set as 1 K/min.

III. RESULTS

Figure 1(a) shows the $\rho_{ab}(T)$ of the underdoped ($T_c = 82$ K) Bi-2223 single crystal (UD1 Bi-2223) near T_c (the results of UD2 Bi-2223 are presented in the Appendix B). Below 100 K, a largely rounded temperature-dependence characteristic of Bi-based copper oxides [22] was observed, whereas tailed behavior was observed at temperatures below 87 K. As $\rho_{ab}(T)$ gradually approached zero, T_c was defined as the temperature

at which $d\rho_{ab}(T)/dT$ became negligibly small ($d\rho_{ab}(T)/dT \approx 0.2 \mu\Omega\text{cm/K}$) (Fig. 1 (b)). The largely rounded temperature dependence was attributed to superconducting fluctuations. This dependence was further analyzed using the formula $\rho_{ab}(T) = 1/(\rho_n(T)^{-1} + \sigma_{2D-AL}(T))$, where $\rho_n(T)$ is the in-plane resistivity in the absence of superconducting fluctuation effects. It is assumed to be $\rho_n(T) = aT + b$ (a and b are constants). $\sigma_{2D-AL}(T)$ is the excess conductivity associated with the 2D Aslamazov—Larkin (AL) superconducting fluctuation [23]. [Here, $\sigma_{2D-AL}(T) = e^2\epsilon^{-1}/16\hbar s$, where ϵ is the reduced temperature, $\epsilon = \ln(T/T_{c0})$, T_{c0} is the mean field, T_c , and s ($= 18.5 \text{ \AA}$) is the distance between the conductive planes.]

At temperatures above 88 K, the fitting reproduced the experimental results well. Thus, T_{c0} was determined as 87 K with a dissociation of 5 K at T_c ($= 82 \text{ K}$). Furthermore, when the applied current was increased to 10 mA, the tailed behavior was enhanced in magnitude at approximately 85 K (inset in Fig. 1 (a)). These results were not attributable to the inhomogeneity of the sample (see Appendix C). Thus, these results implied that the tailed behavior of the in-plane resistivity was owing to a deviation from the mean-field theory, that is, the superconducting fluctuations. The most likely cause was the flux flow resistance owing to the excitation of spontaneous vortices and anti-vortices associated with the KT transition.

The excited free vortex and anti-vortex were all paired at the transition temperature of the KT transition, T_{KT} , such that the electrical resistance was zero at the limit of the zero bias current. However, under a finite bias current, the vortex and the antivortex were pulled apart in opposite directions by the Lorentz force. Consequently, the number n_{free} of free vortices and anti-vortices became finite and resistance was generated. In this case, the relationship between $n_{free} \propto I^{\pi K}$ was derived [24]. Here, K is a constant proportional to the effective superfluid sheet density of the material. Therefore, the following I - V characteristics can be obtained from resistance ($= V/I$) $\propto n_{free}$, $V \propto I^\alpha$ with $\alpha = 1 + \pi K$. At $T = T_{KT}$, K is known to jump from zero to $2/\pi$ upon cooling. Therefore, at $T = T_{KT}$, the power exponent α found in the I - V characteristic jumps to three [24]. This universal jump in the value of α is a phenomenon peculiar to KT transition.

Figure 1(c) shows a log-log plot of the I - V characteristics measured at various temperatures 80-90 K. The data on the low-current side exhibited a linear slope, indicating $V \propto I^\alpha$. The power exponent α was obtained from the slope of the graph. The obtained α was plotted against temperature (Fig. 1 (d)). Above 88 K, the voltage (V) was proportional to the current (I) (i.e., $\alpha = 1$). However, below 87 K, α increased slightly from 1. This is probably because below T_{c0} , free-vortex and anti-vortex excitations occur, some of which pair up and are dissociated by the Lorentz force with increase in the applied current. When the temperature was further reduced, α rapidly increased. Subsequently, α reached three at 81 K, which was slightly lower than T_c ($= 82 \text{ K}$). Thus, we attributed this non-linear I - V characteristics to the KT transition, and defined T_{KT} of this sample as 81 K ($T_{KT} = 81 \text{ K}$).

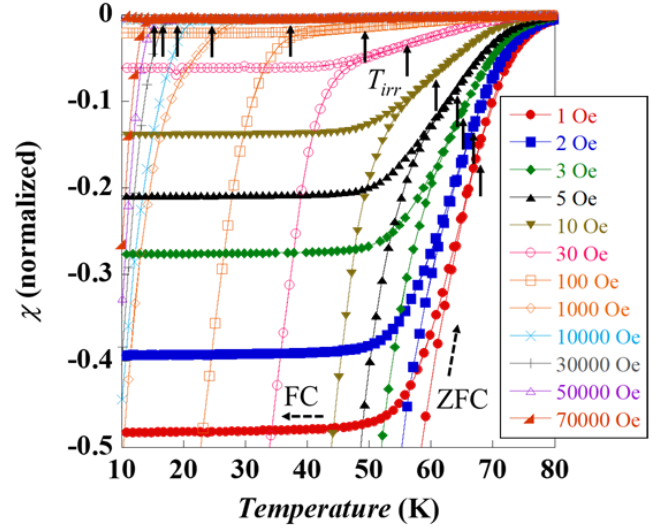


FIG. 2. (Color online) Temperature dependence of magnetic susceptibility (χ) of underdoped (UD) Bi-2223 bulk single crystal under various magnetic fields ($B \parallel c$). Data for the zero-field cooling (ZFC) and cooling in a magnetic field (FC) are indicated via dashed arrows (for 1 Oe data only). χ is normalized by the ZFC value at the lowest temperature. Solid arrows indicate the irreversible temperature (T_{irr}) under the respective magnetic field.

To the best of our understanding, no other explanation may be possible for this observation (Appendix D). However, immediately prior to the occurrence of the KT transition (at a temperature slightly higher than T_{KT}), the system may have been subjected to a normal 3D superconducting transition owing to interplanar interactions. In fact, a finite superconducting current flowed below T_c (see Fig. 9 in the Appendix E).

The KT theory predicts the existence of free vortices and antivortices at $T > T_{KT}$, which facilitates the associated vortex flow resistance. Owing to the vortex flow resistance being proportional to the density of free vortices and anti-vortices, Halperin and Nelson [25] proposed the following equation, $\rho_{ab}(T) = \rho_{ab}^0 \exp(-2ct)$, where c is a constant of the order of 1 and $t = [(T_{c0} - T)/(T - T_{KT})]^{1/2}$. Figure 1(e) shows the $\rho_{ab}(T)$ as a function of t for an applied current of 1 mA. The data were almost on a straight line, indicating that the origin of the tailed $\rho_{ab}(T)$ below 87 K was attributable to the excitation of the free vortices and antivortices.

To generate the vortex/anti-vortex states, the electronic system must be extremely 2D in nature. To confirm this, this study investigated the temperature dependence of the magnetic susceptibility (χ) of underdoped single crystals (UD Bi-2223) annealed under conditions similar to UD2 Bi-2223 under various magnetic fields ($B \parallel c$) (Fig. 2). As shown in the figure, χ did not exhibit hysteresis (i.e., it is reversible) for a wide temperature range (an enlarged view of the data un-

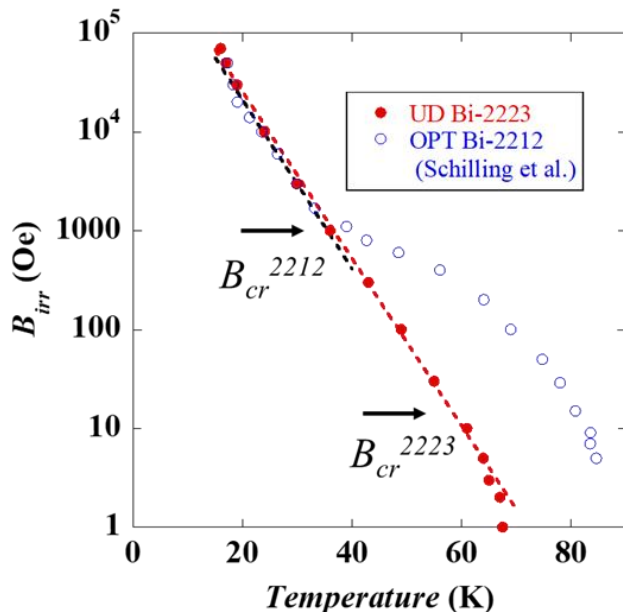


FIG. 3. (Color online) Temperature dependence of the irreversible magnetic field (B_{irr}) for underdoped (UD) Bi-2223 and optimally doped (OPT) Bi-2212 [27]. The vertical axis is shown on a logarithmic scale. The dotted lines indicate the fitting results using the formula, $B_{irr}(T) = B_0 e^{-T/T_0}$, in the low-temperature and high-field region. The crossover fields (B_{cr}) from two to three dimensions are indicated via the arrows for OPT Bi-2212 and UD Bi-2223.

der magnetic fields above 100 Oe is presented in Fig. 10 in the Appendix F). Thus, similar to Bi-2212, UD Bi-2223 had a pancake vortex that reflected the 2D nature of the electronic system, and vortex pinning was extremely weakened [26]. Because the temperature at which the magnetic susceptibility was first observed to exhibit no hysteresis is the irreversible temperature (T_{irr}), the measured magnetic field at that temperature is referred to as the irreversible magnetic field (B_{irr}).

The temperature dependence of B_{irr} is plotted in Fig. 3 on the vertical axis at the log-scale. For comparison, data for optimally doped (OPT) Bi-2212 [27] are also plotted. Plots with other typical copper oxide high- T_c superconductors are presented in Fig. 11 in the Appendix G. Both data exhibited an approximately straight line at high magnetic fields; However, they deviated from a straight line at low magnetic fields. This may be attributed to the crossover of the pancake vortices from a 2D state with decoupling between planes at high fields to a 3D flux lattice state at low fields [26]. Moreover, the deviation from a straight line differed in case of OPT Bi-2212 and UD Bi-2223. The former bent upward whereas the latter bent downward. This is believed to be owing to differences in the anisotropic parameter $\gamma = (m_c/m_{ab})^{1/2}$, where m_c and m_{ab} are the effective quasiparticle masses for tunneling between and motion in the planes. The magnetic field (B_{cr}) that crosses two to three dimensions is theoretically expressed as $B_{cr} \approx \Phi_0/(s\gamma)^2$, where Φ_0 is the flux quantum and s is

the distance between the conduction planes [28]. Further, B_{cr} is defined as the magnetic field at which B_{irr} starts deviating from the high-field linear behavior. From Fig. 3, $B_{cr}(\gamma)$ is $B_{cr}^{2212} \approx 1000$ Oe (≈ 100) and $B_{cr}^{2223} \approx 20$ Oe (≈ 550) for OPT Bi-2212 and UD Bi-2223, respectively. Although the anisotropy of UD Bi-2223 was consistent with the tendency of reported values near the optimal doping for Bi-2223 [29] [that is, $B_{cr}(\gamma)$ is ≈ 1000 Oe (≈ 80), ≈ 600 Oe (≈ 100), and ≈ 300 Oe (≈ 140) for overdoped, optimally doped, and slightly underdoped samples, respectively.], the value appears considerably large.

The anisotropy of cuprate superconductors is generally dependent on doping. The primary reason for this is believed to be the inhomogeneity of the superconducting order parameter in \mathbf{k} -space [30]. In the underdoped state, the large pseudogap opens along the anti-nodal direction [31], resulting in a partial superconducting gap [30, 32]. Consequently, interlayer coupling is suppressed, thereby yielding a large γ . Moreover, the significantly large γ observed in UD Bi-2223 may have been caused by the "nodal metallic state" of the inner CuO_2 plane (IP), which was recently demonstrated using angle-resolved photoemission spectroscopy (ARPES) [33]. Quasiparticles along the nodal direction with robust superconductivity have zero probability of inter-plane tunneling [34]. Therefore, the nodal metallic state of IP may have decoupled the interaction between IP and the outer CuO_2 planes (OP), which resulted in the significantly large γ .

As mentioned above, in the 2D vortex state on the low-temperature, high-field side, B_{irr} exhibits the following relationship:

$$B_{irr}(T) = B_0 e^{-T/T_0}, \quad (1)$$

over a wide temperature range in a material-independent manner, where B_0 and T_0 are constants. However, on the lowest-temperature side, B_{irr} rapidly increases toward the upper critical magnetic field ($B_{c2}(0)$). The parameter values were obtained by fitting Eq. (1) to the appropriate temperature range for each material. The results are listed in Table I in the Appendix H. The fitting was good for all the materials. Therefore, a universal property of copper oxides is that B_{irr} follows Eq. (1) at low temperatures and high magnetic fields.

IV. DISCUSSION

Here, we discuss the origin of the KT transition-like phenomena. Bulk cuprate high- T_c superconductors can be considered as a system of stacked single films with Josephson coupling. Thus, the system can be described by the 3D-XY model [15]. In this case, vortex/anti-vortex excitations occur at each conduction plane below T_{c0} , and the superconducting 3D order at T_c occurs above T_{KT} . Thus, if $T_{KT} \approx T_c \ll T_{c0}$, it can be considered as KT transition-like [14]. According to this theory, the relationship between T_{KT} and T_c was formulated by [15], that is $T_c = T_{KT} + T_{KT}(\pi/\ln \gamma)^2$. We tentatively substituted the parameters obtained for UD1 Bi-2223 ($T_{KT} =$

81 K) and $\gamma = 550$ into this equation to obtain $T_c = 101$ K. This T_c value was considerably higher than T_{KT} and exceeded the observed T_{c0} ($= 87$ K) (Fig. 1 (a)). Thus, the difficulty in inducing the KT transition within the 3D-XY model, as highlighted by Matsuda et al. [14], is also true for underdoped Bi-2223 with a larger anisotropy than OPT Bi-2212.

Therefore, a model beyond the simple 3D-XY model is required. Two sources of force exist between vortices in adjacent planes: Josephson coupling and electromagnetic coupling of the current loops that form the vortices. The 3D-XY model only considers the former. In cases wherein the former is extremely small, the latter becomes dominant. A study [29] found that, in Bi-2223, a crossover occurred from a Josephson-coupling-dominated overdoped state to electromagnetic-coupling-dominated underdoped state in the vicinity of optimal doping. Korshunov [35] demonstrated that the interaction of layers via an electromagnetic field stabilized the vortex lines against the formation of vortex rings and restored the KT transition. Therefore, this model better explains our observations. However, a quantitative evaluation of this model remains challenging.

Alternatively, we considered the in-plane inhomogeneity proposed by Geshkenbein [36] and Ikeda [37] in their analysis of B_{irr} . As shown below, we obtained a result that quantitatively agreed with our observations. Thus, in-plane inhomogeneity is considered as a promising microscopic origin for causing the KT transition-like phenomena in the bulk body.

Geshkenbein et al. assumed that a high T_c ($> T_{c0}$) grain of size R , spacing d , and therefore, areal density $x_G = R^2/d^2$ exists in the normal conducting matrix. When high T_c grains are diluted ($d \gg R$) and placed in a zero magnetic field, the Josephson binding energy (E_J) can be expressed as $E_J(T, \phi) = E_J^0 e^{-d/\xi_n} F_d(\phi)$ [36]; where, $\xi_n = v_F/2\pi T$ is the coherence length of the clean limit normal metal phase and $F_d(\phi)$ is a function representing the phase dependence. The energy scale of the Josephson coupling (E_J^0), assuming 2D nature of the system, is thus obtained $E_J^0 \approx Rv_F(p_F R)N_c/2\pi d^2$, where N_c is the number of conduction planes over which the grains are extended. In Bi-2223, three CuO_2 planes form one conduction plane. In contrast, in Bi-2212, two CuO_2 planes form one conduction plane. N_c is assumed to be ≈ 1 . Considering that the Fermi velocity (v_F) is universal in cuprates [38] and assuming that the p_F (average of three CuO_2 planes) of UD Bi-2223 is not significantly different from that of OPT Bi-2212, the dominant factor of E_J^0 is thus obtained as $x_G (= R^2/d^2)$. Here, we define $T_0 = v_F/2\pi d$, then, $E_J(T, \phi) = E_J^0 e^{-T/T_0} F_d(\phi)$. T_c is expressed as,

$$T_c \approx E_J(T_c), \quad (2)$$

Because the Josephson coupling between grains is significantly suppressed in a magnetic field, a formula equivalent to Eq. (1) was derived for $T > T_0$ [36].

Figure 3 indicates that the slopes (and thus T_0 ; further details are presented in Table I of the Appendix H) of $B_{irr}(T)$ for OPT Bi-2212 and UD Bi-2223 were nearly identical. This facilitates to the estimation of T_c for UD Bi-2223 within

the framework of the model described above, considering OPT Bi-2212's T_c ($= 89$ K). Assuming that superconducting grains are good conductors and normally conducting grains are highly resistive, as well as the distribution of inhomogeneity between these compounds being similar owing to these crystal structures having a common block layer, we can approximate x_G as $x_G \propto \sigma_c$ [39]. From the experimental results, ρ_c of UD Bi-2223 was $85 \Omega\text{cm}$, immediately above T_c (sample a in Fig. 3 of Ref. [40]), and that of OPT Bi-2212 is $7 \Omega\text{cm}$ (sample $\delta = 0.25$ in Fig. 2 of ref. [41]). thus we obtain x_G (thus, E_J^0) of UD Bi-2223 is ≈ 0.08 times that of OPT Bi-2212. Consequently, T_c of UD Bi-2223 was determined to be ≈ 80 K. This value approximately agreed with the observed T_c ($= 82$ K). Thus the shrinking of the superconducting grain and reduction in the energy of the Josephson coupling between grains, resulted in T_c of UD Bi-2223 being significantly lower than its T_{c0} ($= 87$ K). Moreover, they were comparable to T_{KT} ($= 81$ K). Thus, it can be concluded that a KT transition-like phenomenon was observed. In OPT Bi-2212, the larger superconducting grains resulted in larger Josephson coupling energies, and superconductivity possibly occurred immediately below T_{c0} [42].

In fact, nanometer-sized inhomogeneities in the electronic state within the CuO_2 plane have been reported in recent years using scanning tunneling microscopy [43–48]. The gap size was found to be spatially distributed, with regions exhibiting small superconducting gaps. Whereas, regions showing large gaps were in a pseudogap state and were normally conducting. The region exhibiting the superconducting gap was found to shrink as the sample became more underdoped [44], consistent with the numerical analysis using σ_c described above. However, the direct in-plane Josephson properties have rarely been reported [49].

In the previous reports, T_{KT} was much lower (30 and 16 K, in ref. [9] and [12], respectively) than that in this study. What is the origin for the difference? The T_{KT} is the temperature at which the energy loss owing to the dissociation of the vortex-anti-vortex pair was balanced by the gain of the entropy term of the free energy associated with the dissociation. Thus, we obtain $T_{KT} \propto \rho_s^{2D}$, where ρ_s^{2D} is the superfluid sheet density [50]. Therefore, the high T_{KT} of Bi-2223 may be attributable to the larger superfluid density than that of the materials in the literature [9, 12]. The large ρ_s^{2D} in Bi-2223 could be attributed to the fact that the conduction layer of Bi-2223 is composed of a set of three CuO_2 planes.

Here, we exploited the temperature dependence of B_{irr} to estimate B_{cr} , and numerically analyzed B_{irr} for OPT Bi-2212 and UD Bi-2223. We assumed a value close to the vortex-glass transition field B_g of ref. [36]. This assumption was based on the experimental finding for $\text{YBa}_2\text{Cu}_3\text{O}_y$ [51]. However, for accurate discussions on the equilibrium vortex-matter phase diagram in this system, measurements of thermodynamic quantities such as magnetization jumps to indicate vortex-melting [52, 53] or of I - V characteristics to indicate the vortex-glass transition [54] are required. These studies are underway.

We considered the in-plane inhomogeneity as a possible cause of the observed KT transition-like behavior. However, we do not rule out other possibilities such as the Korshunov's model [35]. Furthermore, the data used for this analysis were obtained only from UD Bi-2223. The inner CuO_2 plane, which is unique to Bi-2223, appeared to aid the KT transition by the virtue of extremely flat and enhancing the 2D nature [18, 19]. However, the requirement of the inner CuO_2 plane remains unclear. Furthermore, the extent to which KT transition-like phenomena are universal in cuprates must be investigated by studying material and systematic doping-level dependence in the future.

V. SUMMARY

The KT transition is a topological phase transition specific to a 2D system, and is considered to not occur in bulk (3D) systems. In this study, we revealed a KT transition-like superconducting transition in underdoped Bi-2223 bulk single crystals. The mechanisms governing this phenomena were discussed in terms of extreme 2D nature and/or in-plane inhomogeneity specific to this system. Consequently, the results provided new and compelling evidence that, in copper-oxide high- T_c superconductors, a phase-disordered superconductivity, wherein Cooper pairs exist but their phases do not settle, exists at temperatures higher than T_c . This result constrains the theoretical model on high- T_c superconductivity.

ACKNOWLEDGMENTS

The authors acknowledge the useful discussions with R. Ikeda, Y. Matsuda, S. Adachi, and Y. Itahashi. This work was supported by JSPS KAKENHI Grant Numbers 25400349, 20K03849, and 23K03317. One of the authors (T. W.) was supported by a Hiroasaki University Grant for Distinguished Researchers from fiscal years 2017 to 2018.

Appendix A: Examination of pulse current(I)-voltage(V) characteristics measurement conditions

Measurements of the current(I)-voltage(V) characteristics of a bulk sample and the determination of the power exponent α ($V \propto I^\alpha$) necessitate a current of several tens of mA. Such a large current may cause Joule heating within the sample, even in the case of pulse measurements [55]. Therefore, prior to performing this measurement, we investigated the conditions for the pulse measurement to suppress Joule heating. First, we fixed the pulse period at 1 msec and varied the duty ratio (current pulse width/pulse period) to investigate its effect.

Figure 4(a) shows the temperature dependence of the in-plane resistance (R_{ab}) of the sample. It is an underdoped sample with a superconducting transition temperature (T_c) of 75 K. The $I - V$ characteristics were measured at various duty

ratios at 77 K, that is immediately above T_c (Fig. 4(b)). As the duty ratio increased, the nonlinearity increased. Thus, an increase in the duty ratio caused the effect of heat generation to become more pronounced. The results were plotted against the voltage (V) on the vertical axis and the duty ratio on the horizontal axis for various current values (Fig. 4(c)). At any current value, the voltage (V) increased approximately linearly with the duty ratio. Therefore, the V values obtained by extrapolating this straight line to a duty ratio of zero were considered as the true voltages in the absence of heat generation. The $I - V$ characteristics at a duty ratio of zero and those at a duty ratio of 5 % are plotted in Fig. 4(d). The two almost overlapped, and the power exponents α were also approximately the same ($\alpha = 1.93$ and $\alpha = 1.90$ for the duty ratios of 5 % and 0 %, respectively). Therefore, we considered that the data with a duty ratio of 5 % sufficiently suppressed the heat generation. Figure 4(e) shows the $I - V$ characteristics near T_c , measured under this condition. On the high-temperature side, it was approximately Ohmic ($\alpha = 1$); however, α increased as the temperature decreased, reaching $\alpha = 3$ near T_c ($= 75$ K).

However, as shown in Fig. 4(e), the data on the low current side were slightly noisy. Therefore, to improve the data signal to noise (S/N) ratio, we extended the pulse period while maintaining the duty ratio below 5 %. Specifically, the $I - V$ characteristics were examined by varying the pulse period across 50-500 ms and the duty ratio across 0.2-2 % (Fig. 4(f)). Because there was no difference in the data under any condition, the effect of heat generation was considered negligible under these conditions. Consequently, the measurement conditions were set to a pulse period of 50 ms and duty ratio of 2 %.

Appendix B: Transport properties of the UD2 Bi-2223 sample

Figure 5(a) shows the temperature dependence of the temperature derivative of the zero-field in-plane resistivity $d\rho_{ab}(T)/dT$ for the UD2 Bi-2223 sample. Consequently, we determined $T_c = 78$ K, according to the definition in the text.

Figure 5(b) shows its $I - V$ characteristics. On the high-temperature side, it was approximately Ohmic ($\alpha = 1$); however, α increased with decreasing temperature, reaching $\alpha = 3$ near T_c ($= 78$ K) ($T_{KT} = 78$ K). Figure 5(c) shows the temperature dependence of α thus obtained. Notably, the $I - V$ characteristics were S -shaped below 84 K. The S -shaped behavior has already been presented in the main text (Fig. 1(c)); however, the behavior was more pronounced (Fig. 5(b)). This behavior is similar to that of 2D MoS_2 with carrier injection owing to the electric field effect [56]. In the low-current regime, the voltage increased significantly with an increase in the dissociated vortex and antivortex pairs as the current increased. As the current was further increased, a phase slip line formed, the viscous force against the vortex (anti-vortex) weakened, the velocity of the vortex (anti-vortex) increased, and the voltage increased further [57]. However, at higher currents, the vortex (anti-vortex) disappeared and approached the $I - V$ characteristics of the normal state. Therefore, the S -shaped behav-

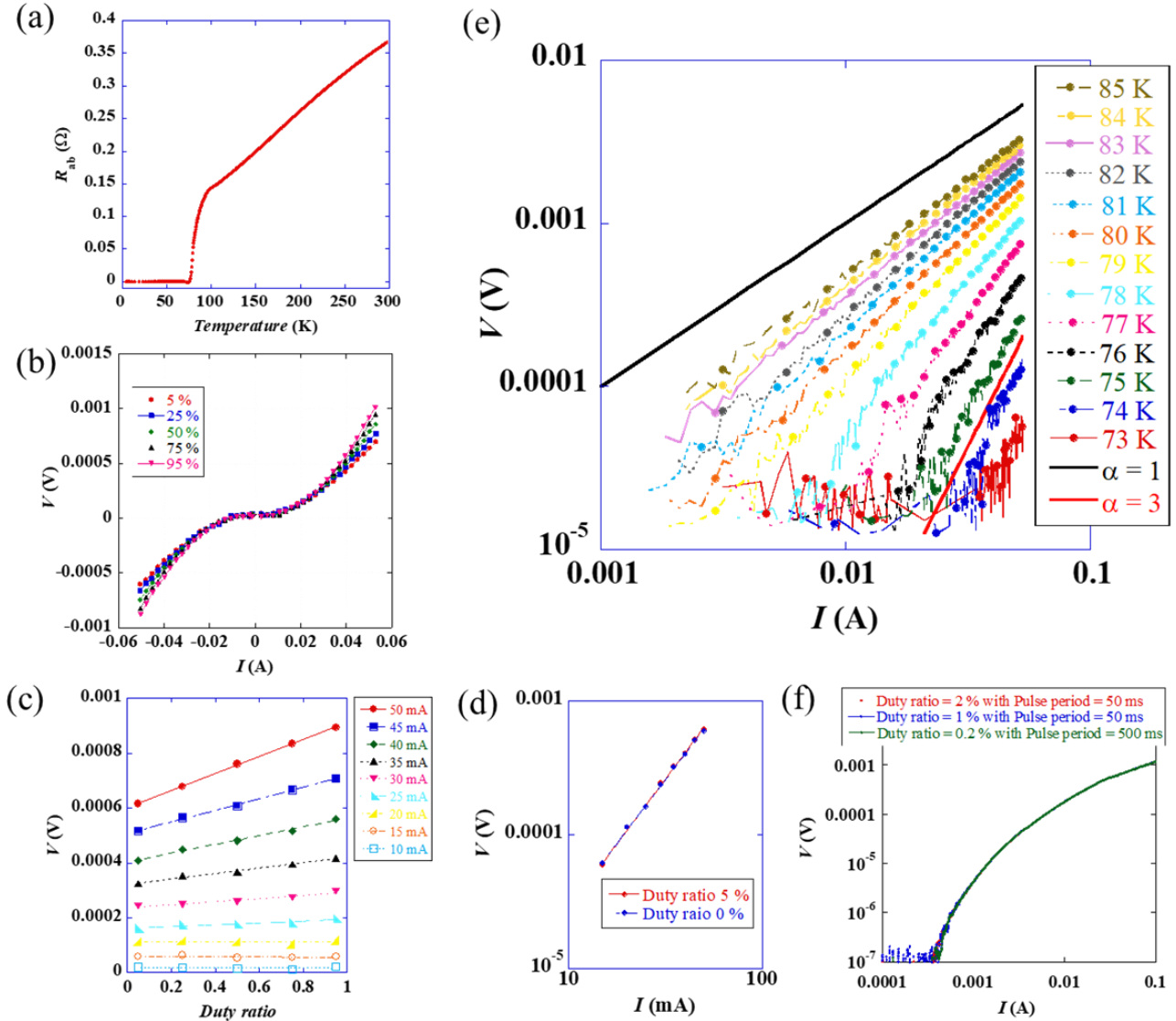


FIG. 4. (Color online) (a) Temperature dependence of the in-plane resistance (R_{ab}) of underdoped Bi-2223 single crystal used to examine the measurement conditions of pulsed $I - V$ characteristics ($T_c = 75$ K). (b) Measured $I - V$ characteristics at various duty ratios at 77 K. (c) Voltage (V) vs. duty ratio for various current values. (d) Comparison of $I - V$ characteristics at a hypothetical duty ratio of zero and $I - V$ characteristics at a duty ratio of 5%. The two almost overlap. (e) $I - V$ characteristics near T_c measured under a duty ratio of 5%. (f) $I - V$ characteristics measured under various conditions with extended pulse period. Measurements are performed at the superconducting state (60 K) for an underdoped Bi-2223 single crystal different from the sample shown in (a).

ior was considered a characteristic of systems that undergo KT transition. The observation of a behavior similar to that of two-dimensional MoS_2 with a certain KT transition indicated that the UD1 and UD2 Bi-2223 used in this study also cause the excitation of vortices and anti-vortices similar to the KT transition.

Figure 5(d) shows the temperature dependence of the in-plane resistivity (ρ_{ab}) with and without magnetic fields and the fitting results based on theory. An analysis of the zero-magnetic-field data revealed the mean-field superconducting

transition temperature (T_{c0}) as 84 K. The data in the magnetic field were analyzed using the theory formulated by Ikeda-Ohmi-Tsuneto (IOT theory) [58]. We previously performed a similar analysis for Bi-2223 and Bi-2212 near the optimum doping (further details on the analysis method can be found in [22]). Because the theoretical formula includes the specific heat jump (ΔC), in-plane and inter-plane coherence lengths (ξ_{ab} and ξ_c , respectively), and T_{c0} as parameters, they can be evaluated by fitting the transition curves in the magnetic fields. Here, fitting was performed with ξ_c fixed at $\xi_c = 0.1$ \AA be-

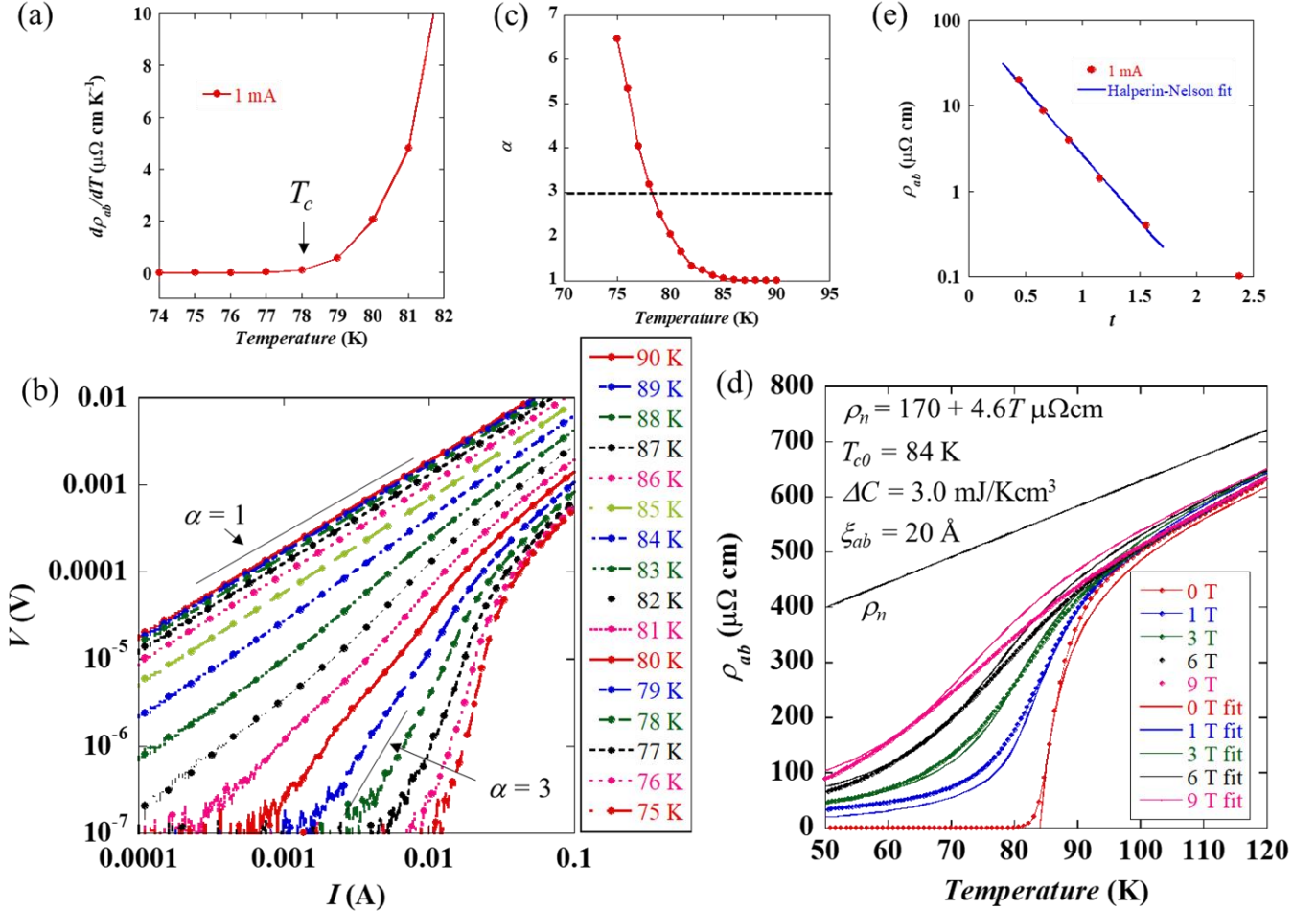


FIG. 5. (Color online) (a) Temperature derivative of zero-field in-plane resistivity ($d\rho_{ab}(T)/dT$) vs. temperature. (b) I - V characteristics near T_c ($= 78$ K). (c) Temperature dependence of the power exponent α . (d) Temperature dependence of ρ_{ab} with and without magnetic fields, and their fitting results using IOT theory. (e) Temperature dependence of ρ_{ab} at $T_{KT} < T < T_{c0}$. The straight line indicates the fitting result using the Halperin-Nelson equation, $\rho_{ab}(T) = \rho_{ab}^0 \exp(-2ct)$, where $t = [(T_{c0} - T)/(T - T_{KT})]^{1/2}$, with $\rho_{ab}^0 = 90 \mu\Omega\text{cm}$ and $c = 1.76$.

TABLE I. Parameter values determined by fitting the irreversible magnetic field ($B_{irr}(T)$) for various cuprate high- T_c superconductors.

	UD Bi-2223	OPT Bi-2212	Tl 2201	LSCO ($p = 0.07$)	YBCO ($p = 0.132$)	YBCO ($p = 0.116$)	YBCO ($p = 0.108$)
B_0 (T)	129	108	9.2	28	44	38	44
T_0 (K)	5.1	5.1	3.5	1.8	17	10	8.2

cause even if ξ_c was reduced further, the fitting curve did not change. From the fitting, ξ_{ab} was obtained as ≈ 20 Å. Thus, the anisotropy parameter (γ) was determined as $\gamma = \xi_{ab}/\xi_c \geq 200$. This result was consistent with the value of γ (≈ 550) obtained by evaluating the crossover magnetic field (B_{cr}) in the main text. Furthermore, $\Delta C \approx 3.0$ mJ/Kcm³ was obtained. This value was considerably smaller than that of optimally doped Bi-2212 ($\Delta C \approx 20.0$ mJ/Kcm³) [22]. The superfluid density (ρ_s) (phase stiffness) is related to the magnetic field penetration depth (λ_L) as $\rho_s \propto 1/\lambda_L^2$. Further, λ_L is related to

ΔC as $1/\lambda_L^2 = 32\pi^3 \xi_{ab}^2 T_{c0} \Delta C / \Phi_0^2$ (where Φ_0 is the magnetic flux quantum) [58]. Using these relations, we estimated $1/\lambda_L^2$ as $23.4 \mu\text{m}^{-2}$ and $44.1 \mu\text{m}^{-2}$ for UD2 Bi-2223 and optimally doped Bi-2212 [22], respectively. Thus, underdoped Bi-2223 has a smaller ρ_s than optimally doped Bi-2212. This renders it difficult for Cooper pairs to be coherent in phase, and thus underdoped Bi-2223 is more likely to undergo KT transition-like phenomena.

Figure 5(e) presents the tailored temperature dependence of ρ_{ab} below T_{c0} (84 K). The data are approximately on a straight

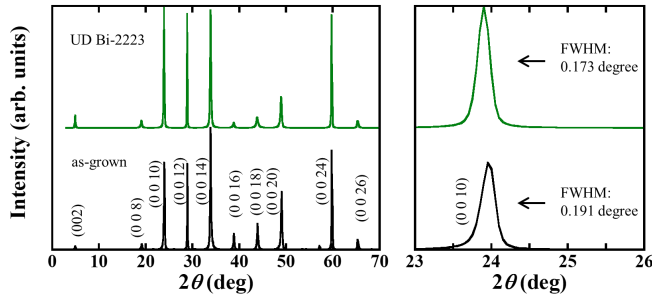


FIG. 6. (Color online) X-ray diffraction (XRD) patterns of as-grown and UD Bi-2223 single crystals.

line. Thus, as shown in Fig. 1(e) in the main text, the tailed ρ_{ab} was owing to the free-vortex and anti-vortex excitations.

Appendix C: Information on the quality of the samples

Figure 6 shows the X-ray diffraction patterns of an as-grown sample and an underdoped sample (UD Bi-2223) prepared under the same annealing conditions as that in the case of UD2 Bi-2223. They are obtained from the same Bi-2223 crystal rod used in this study. In both cases, only the peak of (0 0 2n) of Bi-2223 was observed; thus, it had a high-purity Bi-2223 single crystal with little contamination of Bi-2212. As the crystal is a sample with excellent orientation, there is no contamination with other impurities. Owing to the full width at half maximum (FWHM) being narrower in the annealed sample than in the as-grown sample, it can be concluded that there is no problem of macroscopic oxygen inhomogeneity associated with annealing. The narrowing of the FWHM with annealing is reproducible [21].

Figure 7 shows the temperature dependence of the resistivity ρ_{ab} of (a) UD1 Bi-2223 and its (b) as-grown crystal with various bias currents. For comparison, the temperature on the horizontal axis was plotted at the same width, and the resistivity on the vertical axis was plotted on the same scale. In the UD1 Bi-2223 crystal, a noticeable tailing behavior was evident. Further, the tailing behavior was enhanced in magnitude at the temperature intervals with increasing the bias currents. The non-ohmic resistance cannot be explained by the non-uniformity of the crystal. Furthermore, in the as-grown crystal, the tailing behavior and the non-ohmicity were suppressed. The FWHM of the X-ray diffraction pattern implied that the crystallinity of the as-grown crystal was more disordered than that of the annealed crystal. The suppressed tailing behavior and the non-ohmicity in the disordered as-grown crystal strongly indicated that the anomalies observed in the UD1 Bi-2223 crystal were not due to crystalline inhomogeneity.

Figure 8 shows a transmission electron microscope (TEM)

image of a Bi-2223 single crystal wherein only the (0 0 2n) peaks of Bi-2223 were observed in the XRD pattern, as in Fig. 6 (and therefore had the same quality as the sample used in this study), taken with an electron beam incident in the b -axis direction [20]. No stacking faults were observed. A slight (approximately 2 %) intergrowth of Bi-2212 was observed. However, these intergrowths did not affect the results of this study. This is because the T_c of the Bi-2223 is considerably higher than that of the Bi-2212.

Appendix D: Why we attribute the change of α from 1 to 3 to the KT transition

We have observed the change of α from one to three in Fig. 1(d) in the main text. We conclude that this phenomenon is owing to the KT transition as follows.

Similar I - V characteristics have been reported in cuprate superconductors [54]. However, this phenomenon pertains specifically to the vortex glass transition in a magnetic field, and fundamentally differs from the zero-field phenomenon being investigated in this study. Further, it has been reported that the I - V characteristics follow a power-law behavior at the glass transition temperature ($T = T_g$); however, the power exponent α is not necessarily three (for YBCO, $2.5 < \alpha < 3.0$ [26], and for Bi-2223, $\alpha < 1.0$ [59]). Furthermore, this power-law behavior does not hold in the temperature range above and below the transition temperature.

For superconducting practical wires, the power exponent n -value of the I - V characteristic ($V \propto I^n$) indicates how rapidly the I - V curve increases after exceeding the critical current value ($I_c \approx 50$ -100 A) at temperatures below T_c . However, under normal conditions (in the absence of serious damage owing to bending stress, tensile strain, etc.), $n \approx 10 - 60$ [60].

Therefore, in this study, the change in α from one to three near T_c under zero magnetic field is sufficient evidence for the occurrence of KT transition without any other interpretation.

Appendix E: Appearance of a critical current (I_c) and evolution of α below T_c

For convenience, we estimated α via power law fitting for the I - V characteristics ($V \propto I^\alpha$) below T_c in the same manner as above T_c (see, Fig. 1(d) in the main text and Fig. 5(c) in the Appendix B). However, notably, the obtained α below T_c was only an approximate value for the following reasons:

Figure 9(a) and 9(b) show the I - V characteristics in the low bias current (I) and low voltage (V) regimes for the UD1 Bi-2223 and UD2 Bi-2223 samples, respectively. As evident, I_c appeared below T_c . Therefore, the power-law fitting was not exact. Thus, the fact that α reached three below or near T_c does not necessarily imply the occurrence of a true KT transition. This may have resulted in that α does not "jump" to 3 in this study. Here, the 3D superconducting transition occurred

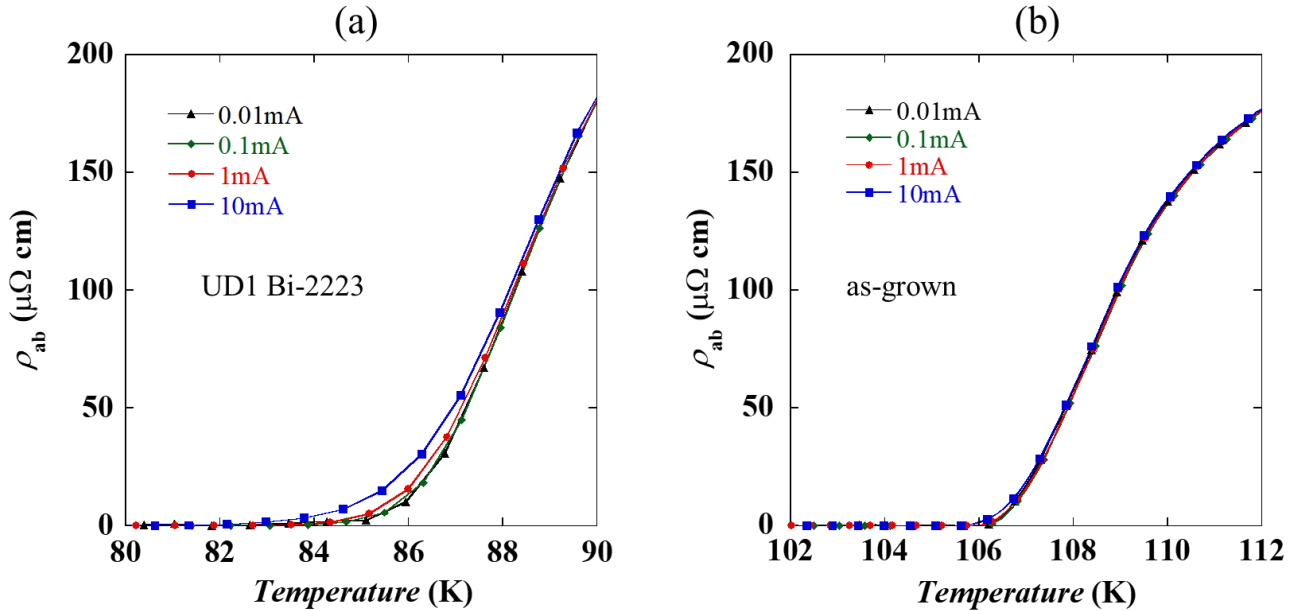


FIG. 7. (Color online) In-plane resistivity ρ_{ab} of (a) an underdoped (UD1) and (b) as-grown Bi-2223 single crystals with various applied currents.

at T_c , immediately above the "hypothetical" T_{KT} at which α reached 3.

Appendix F: Magnified view of temperature dependence of magnetic susceptibility

Figure 10 shows an enlarged view of the region with low magnetic susceptibility to facilitate the easier observation of the high-magnetic-field data in Fig. 2 in the main text. As evident, hysteresis was observed even upon the application of a high magnetic field, and the irreversible temperature (T_{irr}) could be defined. However, the data for cooling in a magnetic field (FC) changed in the opposite direction (increasing with decreasing temperature). The cause of this phenomenon is not well-understood.

Appendix G: B_{irr} vs. T with other typical copper oxide high- T_c superconductors

Figure 11 presents plots of B_{irr} vs. T for typical copper oxide high- T_c superconductors, UD Bi-2223 (this study), optimally doped (OPT) Bi-2212 [27], $Tl_2Ba_2CuO_6 + \delta$ (Tl-2201) [61], LSCO ($p = 0.07$) [62], and YBCO ($p = 0.132, 0.116, 0.108$) [63]. Here, irreversible fields and vortex-lattice melting fields were not distinguished. Moreover, the methods for determining B_{irr} varied, depending on the literature. Nevertheless, all data were almost on a straight line at high mag-

netic fields, but deviated from a straight line at low magnetic fields. Therefore, this activation type behavior for B_{irr} may be universal in cuprates.

Appendix H: Parameter values determined by fitting the irreversible magnetic field ($B_{irr}(T)$)

Table I lists the parameter values determined by fitting the irreversible magnetic field ($B_{irr}(T)$) of various cuprate high- T_c superconductors exhibited in Fig. 11. The fitting was performed using the formula $B_{irr}(T) = B_0 e^{-T/T_0}$. UD Bi-2223 and OPT Bi-2212 had the same T_0 .

* Present address: Physics Department, College of Engineering, Nihon University, Fukushima 963-8642, Japan. E-mail address: watanabe.takao@nihon-u.ac.jp

- [1] Y. J. Uemura, G. M. Luke, B. J. Sternlieb, J. H. Brewer, J. F. Carolan, W. N. Hardy, R. Kadono, J. R. Kempton, R. F. Kiefl, S. R. Kreitzman, P. Mulhern, T. M. Riseman, D. L. Williams, B. X. Yang, S. Uchida, H. Takagi, J. Gopalakrishnan, A. W. Sleight, M. A. Subramanian, C. L. Chien, M. Z. Cieplak, G. Xiao, V. Y. Lee, B. W. Statt, C. E. Stronach, W. J. Kossler, and X. H. Yu, Universal Correlations between T_c , and n_s/m^* (Carrier Density over Effective Mass) in High- T_c , Cuprate Superconductors, Phys. Rev. Lett. **62**, 2317 (1989).

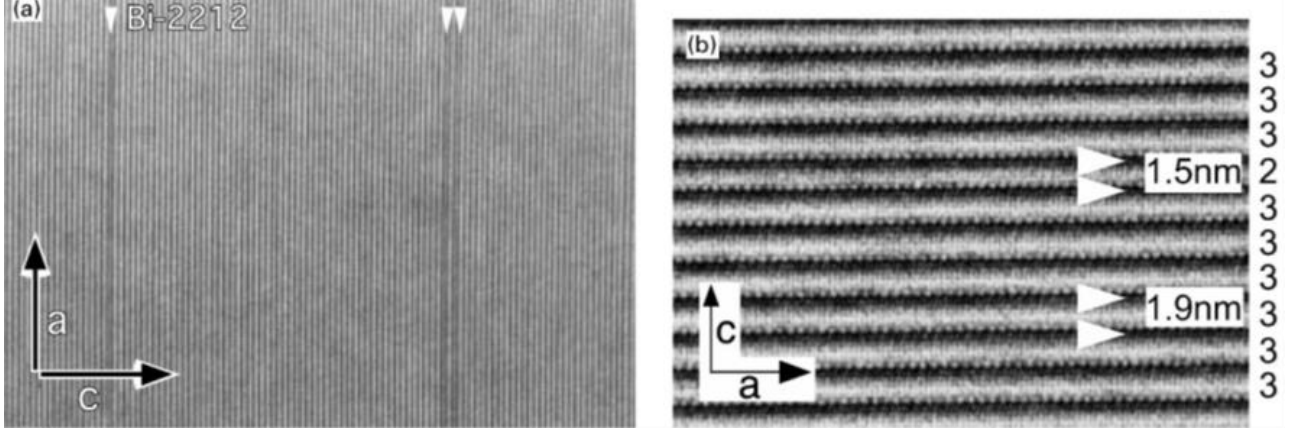


FIG. 8. (Color online) (a) TEM image of a Bi-2223 single crystal, captured with the incident beam parallel to the b direction. (b) The scale is expanded to show the intergrowth of Bi-2212. Bi-2212 marked as “2” is intergrown in the Bi-2223 marked as “3”. The data is reproduced with permission from ref. [20].

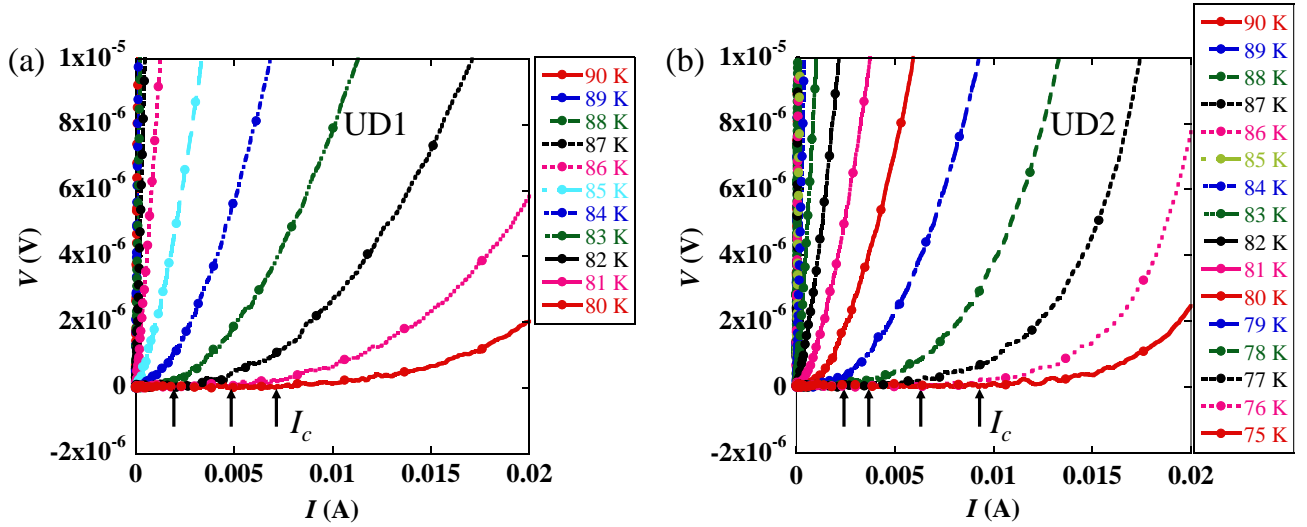


FIG. 9. (Color online) Expanded I - V characteristics plotted as linear scales for (a) UD1 Bi-2223 and (b) UD2 Bi-2223. The arrows indicate I_c s for each temperatures. I_c is defined as the current at which V becomes below 1×10^{-8} V (noise level). (a) I_c is 0.0020 ± 0.0005 , 0.0048 ± 0.0005 , and 0.0071 ± 0.0010 A for 82 ($= T_c$), 81, and 80 K, respectively. (b) I_c is 0.0026 ± 0.0005 , 0.0038 ± 0.0005 , 0.0063 ± 0.0010 , and 0.0092 ± 0.0010 A for 78 ($= T_c$), 77, 76, and 75 K, respectively.

[2] V. J. Emery and S. A. Kivelson, Importance of phase fluctuations in superconductors with small superfluid density, *Nature* **374**, 434 (1995).

[3] M. Franz and A. J. Millis, Phase fluctuations and spectral properties of underdoped cuprates, *Phys. Rev. B* **58**, 14572 (1998).

[4] Z. A. Xu, N. P. Ong, Y. Wang, T. Kakeshita, and S. Uchida, Vortex-like excitations and the onset of superconducting phase fluctuation in underdoped $\text{La}_{2-x}\text{Sr}_x\text{CuO}_4$, *Nature* **406**, 486 (2000).

[5] Y. Wang, L. Li, M. J. Naughton, G. D. Gu, S. Uchida, and N. P. Ong, Field-Enhanced Diamagnetism in the Pseudogap State

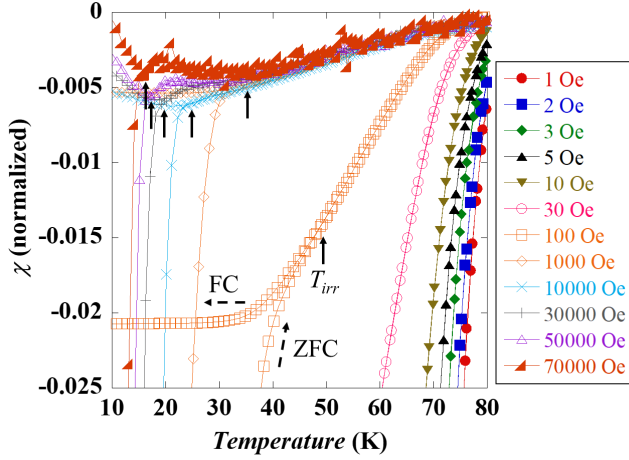


FIG. 10. (Color online) Enlarged view of the region of the low magnetic susceptibility in Fig. 2 in the main text. Hysteresis is observed even upon the application of a high magnetic field, and an irreversible temperature (T_{irr}) can be defined. The arrows indicate T_{irr} under the respective applied magnetic fields.

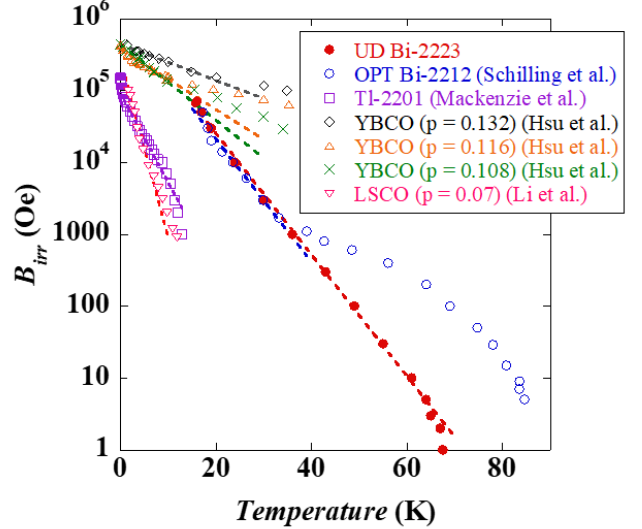


FIG. 11. (Color online) Temperature dependence of the irreversible magnetic field (B_{irr}) for underdoped (UD) Bi-2223, optimally doped (OPT) Bi-2212 [27], $Tl_2Ba_2CuO_6 + \delta$ (Tl-2201) [61], LSCO ($p = 0.07$) [62], and YBCO ($p = 0.132, 0.116, 0.108$) [63]. The vertical axis is shown on a logarithmic scale. The dotted lines indicate the fitting results using the formula, $B_{irr}(T) = B_0 e^{-T/T_0}$, on the low-temperature and high-field region.

of the Cuprate $Bi_2Sr_2CaCu_2O_{8+\delta}$ Superconductor in an Intense Magnetic Field, Phys. Rev. Lett. **95**, 247002 (2005).

- [6] J. M. Kosterlitz and D. J. Thouless, Ordering, metastability and phase transitions in two-dimensional systems, J. Phys. C **6**, 1181 (1973).
- [7] M. R. Beasley, J. E. Mooij, and T. P. Orlando, Possibility of Vortex-Antivortex Pair Dissociation in Two-Dimensional Superconductors, Phys. Rev. Lett. **42**, 1165 (1979).
- [8] M. Franz, Importance of fluctuations, Nature Phys. **3**, 686 (2007).
- [9] Y. Matsuda, S. Komiyama, T. Terashima, K. Shimura, and Y. Bando, Disappearance of Hall Resistance in One-Unit-Cell-Thick $YBa_2Cu_3O_{7-\delta}$: Evidence of Free Vortex-Antivortex Excitation, Phys. Rev. Lett. **69**, 3228 (1992).
- [10] I. Hetel, T. R. Lemberger, and M. Randeria, Quantum critical behaviour in the superfluid density of strongly underdoped ultrathin copper oxide films, Nature Phys. **3**, 700 (2007).
- [11] A. B. Yu, Z. Huang, W. Peng, H. Li, C. T. Lin, X. F. Zhang, and L. X. You, Fabrication and transport properties of two dimensional $Bi_2Sr_2Ca_2Cu_3O_{10+\delta}$ micro-bridge, Appl. Phys. Lett. **120**, 072601 (2022).
- [12] Q. Li, M. Hücker, G. D. Gu, A. M. Tsvelik, and J. M. Tranquada, Two-Dimensional Superconducting Fluctuations in Stripe-Ordered $La_{1.875}Ba_{0.125}CuO_4$, Phys. Rev. Lett. **99**, 067001 (2007).
- [13] H. Kitano, T. Ohashi, A. Maeda, and I. Tsukada, Critical microwave-conductivity fluctuations across the phase diagram of superconducting $La_{2-x}Sr_xCuO_4$ thin films, Phys. Rev. B **73**, 092504 (2006).
- [14] Y. Matsuda, S. Komiyama, T. Onogi, T. Terashima, K. Shimura, and Y. Bando, Thickness dependence of the Kosterlitz-Thouless transition in ultrathin $YBa_2Cu_3O_{7-\delta}$ films, Phys. Rev. B **48**, 10498 (1993).
- [15] S. Hikami and T. Tsuneto, Phase Transition of Quasi-Two Dimensional Planar System, Prog. Theor. Phys. **63**, 387 (1980).
- [16] H. Mukuda, S. Shimizu, A. Iyo, , and Y. Kitaoka, High- T_c Superconductivity and Antiferromagnetism in Multilayered Copper Oxides —A New Paradigm of Superconducting Mechanism—, J. Phys. Soc. Jpn. **81**, 011008 (2012).
- [17] S. Kunisada, S. Isono, Y. Kohama, S. Sakai, C. Bareille, S. Sakuragi, R. Noguchi, K. Kurokawa, K. Kuroda, Y. Ishida, S. Adachi, R. Sekine, T. K. Kim, C. Cacho, S. Shin, T. Tohyama, K. Tokiwa, and T. Kondo, Observation of small Fermi pockets protected by clean CuO_2 sheets of a high- T_c superconductor, Science **369**, 833 (2020).
- [18] T. Iye, T. Nagatochi, R. Ikeda, and A. Matsuda, Diamagnetism above T_c in Underdoped $Bi_{2.2}Sr_{1.8}Ca_2Cu_3O_{10+\delta}$, J. Phys. Soc. Jpn. **79**, 114711 (2010).
- [19] Y. Nomura, R. Okamoto, T. A. Mizuno, S. Adachi, T. Watanabe, M. Suzuki, and I. Kakeya, Role of the inner copper oxide plane in interlayer Josephson effects in multilayered cuprate superconductors, Phys. Rev. B **100**, 144515 (2019).
- [20] T. Fujii, T. Watanabe, and A. Matsuda, Single-crystal growth of $Bi_2Sr_2Ca_2Cu_3O_{10+\delta}$ (Bi-2223) by TSFZ method, J. Cryst. Growth **223**, 175 (2001).
- [21] S. Adachi, T. Usui, K. Takahashi, K. Kosugi, T. Watanabe, T. Nishizaki, T. Adachi, S. Kimura, K. Sato, K. M. Suzuki, M. Fujita, and K. Y. and T. Fujii, Single-crystal growth of underdoped Bi-2223, Physics Procedia **65**, 53 (2015).
- [22] S. Adachi, T. Usui, Y. Ito, H. Kudo, H. Kushibiki, K. Murata, T. Watanabe, K. Kudo, T. Nishizaki, N. Kobayashi, S. Kimura, M. Fujita, K. Yamada, T. Noji, Y. Koike, and T. Fujii, Unscaling Superconducting Parameters with T_c for Bi-2212 and Bi-2223: A Magnetotransport Study in the Superconductive Fluctuation Regime, J. Phys. Soc. Jpn. **84**, 024706 (2015).
- [23] L. G. Aslamasov and A. I. Larkin, The influence of fluctuation pairing of electrons on the conductivity of normal metal, Phys.

- Lett. A **26**, 238 (1968).
- [24] A. M. Kadin, K. Epstein, and A. M. Goldman, Renormalization and the Kosterlitz-Thouless transition in a two-dimensional superconductor, *Phys. Rev. B* **27**, 6691 (1983).
- [25] B. I. Halperin and D. R. Nelson, Resistive Transition in Superconducting Films, *J. Low Temp. Phys.* **36**, 599 (1979).
- [26] G. Blatter, M. Y. Feigel'man, Y. B. Geshkenbein, A. I. Larkin, and V. M. Vinokur, Vortices in high-temperature superconductors, *Rev. Mod. Phys.* **66**, 1125 (1994).
- [27] A. Schilling, R. Jin, J. D. Guo, and H. R. Ott, Irreversibility Line of Monocrystalline $\text{Bi}_2\text{Sr}_2\text{CaCu}_2\text{O}_8$: Experimental Evidence for a Dimensional Crossover of the Vortex Ensemble, *Phys. Rev. Lett.* **71**, 1899 (1993).
- [28] V. M. Vinokur, P. H. Kes, and A. E. Koshelev, Flux pinning and creep in very anisotropic high temperature superconductors, *Physica C* **168**, 29 (1990).
- [29] A. Piriou, Y. Fasano, E. Giannini, and O. Fischer, Effect of oxygen-doping on $\text{Bi}_2\text{Sr}_2\text{Ca}_2\text{Cu}_3\text{O}_{10+\delta}$ vortex matter: Crossover from electromagnetic to Josephson interlayer coupling, *Phys. Rev. B* **77**, 184508 (2008).
- [30] M. Suzuki, T. Hamatani, K. Anagawa, and T. Watanabe, Evolution of interlayer tunneling spectra and superfluid density with doping in $\text{Bi}_2\text{Sr}_2\text{CaCu}_2\text{O}_{8+\delta}$, *Phys. Rev. B* **85**, 214529 (2012).
- [31] S Hüfner, M A Hossain, A Damascelli, and G A Sawatzky, Two gaps make a high-temperature superconductor?, *Rep. Prog. Phys.* **71**, 062501 (2008).
- [32] M. R. Norman, H. Ding, M. Randeria, J. C. Campuzano, T. Yokoya, T. Takahashi, T. Takeuchi, T. Mochiku, K. Kadowaki, P. Guptasarma, and D. G. Hinks, Destruction of the Fermi surface in underdoped high- T_c superconductors, *Nature* **392**, 157 (1998).
- [33] S. Ideta et al., unpublished.
- [34] L. B. Ioffe and A. J. Millis, Zone-diagonal-dominated transport in high- T_c cuprates, *Phys. Rev. B* **58**, 11631 (1998).
- [35] S. E. Korshunov, Vortex Rings and Phase Transition in Layered-Lattice Superconductors, *Europhys. Lett.* **11(8)**, 757 (1990).
- [36] V. B. Geshkenbein, L. B. Ioffe, and A. J. Millis, Theory of the Resistive Transition in Overdoped $\text{Tl}_2\text{Ba}_2\text{CuO}_{6+\delta}$: Implications for the Vortex Viscosity and the Quasiparticle Scattering Rate in High- T_c Superconductors, *Phys. Rev. Lett.* **80**, 5778 (1998).
- [37] R. Ikeda, Superconducting transition in disordered granular superconductors in magnetic fields, *Phys. Rev. B* **74**, 054510 (2006).
- [38] X. J. Zhou, T. Yoshida, A. Lanzara, P. V. Bogdanov, S. A. Kellar, K. M. Shen, W. L. Yang, F. Ronning, T. Sasagawa, T. Kakeshita, T. Noda, H. Eisaki, S. Uchida, C. T. Lin, F. Zhou, J.W. Xiong, W. X. Ti, Z. X. Zhao, A. Fujimori, Z. Hussain, and Z.-X. Shen, Universal nodal Fermi velocity, *Nature* **423**, 398 (2003).
- [39] Y. Yamada, K. Anagawa, T. Shibauchi, T. Fujii, T. Watanabe, A. Matsuda, and M. Suzuki, Interlayer tunneling spectroscopy and doping-dependent energy-gap structure of the trilayer superconductor $\text{Bi}_2\text{Sr}_2\text{Ca}_2\text{Cu}_3\text{O}_{10+\delta}$, *Phys. Rev. B* **68**, 054533 (2003).
- [40] T. Fujii, I. Terasaki, T. Watanabe, and A. Matsuda, Doping dependence of anisotropic resistivities in the trilayered superconductor $\text{Bi}_2\text{Sr}_2\text{Ca}_2\text{Cu}_3\text{O}_{10+\delta}$, *Phys. Rev. B* **66**, 024507 (2002).
- [41] T. Watanabe, T. Fujii, and A. Matsuda, Pseudogap in $\text{Bi}_2\text{Sr}_2\text{CaCu}_2\text{O}_{8+\delta}$ Studied by Measuring Anisotropic Susceptibilities and Out-of-Plane Transport, *Phys. Rev. Lett.* **84**, 5848 (2000).
- [42] S. Martin, A. T. Fiory, R. M. Fleming, G. P. Espinosa, and A. S. Cooper, Vortex-Pair Excitation near the Superconducting Transition of $\text{Bi}_2\text{Sr}_2\text{CaCu}_2\text{O}_8$ Crystals, *Phys. Rev. Lett.* **62**, 677 (1989).
- [43] S. H. Pan, J. P. O'Neal, R. L. Badzey, C. Chamon, H. Ding, J. R. Engelbrecht, Z. Wang, H. Eisaki, S. Uchida, A. K. Gupta, K.-W. Ng, E. W. Hudson, K. M. Lang, and J. C. Davis, Microscopic electronic inhomogeneity in the high- T_c superconductor $\text{Bi}_2\text{Sr}_2\text{CaCu}_2\text{O}_{8+x}$, *Nature* **413**, 282 (2001).
- [44] K. M. Lang, V. Madhavan, J. E. Hoffman, E. W. Hudson, H. Eisaki, S. Uchida, and J. C. Davis, Imaging the granular structure of high- T_c superconductivity in underdoped $\text{Bi}_2\text{Sr}_2\text{CaCu}_2\text{O}_{8+\delta}$, *Nature* **412**, 412 (2002).
- [45] K. K. Gomes, A. N. Pasupathy, A. Pushp, S. Ono, Y. Ando, and A. Yazdani, Visualizing pair formation on the atomic scale in the high- T_c superconductor $\text{Bi}_2\text{Sr}_2\text{CaCu}_2\text{O}_{8+\delta}$, *Nature* **447**, 569 (2007).
- [46] T. Kasai, H. Nakajima, T. Fujii, I. Terasaki, T. Watanabe, H. Shibata, and A. Matsuda, High- T_c superconductor near the $S-I$ transition, *Physica C* **469**, 1016 (2009).
- [47] M. H. Hamidian, S. D. Edkins, S. H. Joo, A. Kostin, H. Eisaki, S. Uchida, M. J. Lawler, E.-A. Kim, A. P. Mackenzie, K. Fujita, J. Lee, and J. C. Davis, Detection of a Cooper-pair density wave in $\text{Bi}_2\text{Sr}_2\text{CaCu}_2\text{O}_{8+x}$, *Nature* **532**, 343 (2016).
- [48] Z. Du, H. Li, S. H. Joo, E. P. Donoway, J. Lee, J. C. Davis, G. Gu, P. D. Johnson, and K. Fujita, Imaging the energy gap modulations of the cuprate pair-density-wave state, *Nature* **580**, 65 (2020).
- [49] K. Semba, M. Mukaida, and A. Matsuda, TRANSPORT PROPERTY AND QUANTUM CRITICAL POINT OF UNDERDOPED $\text{YBa}_2\text{Cu}_3\text{O}_{6+x}$ in *Proceedings of the Mass and Charge Transport in Inorganic Materials: Fundamentals to Devices, Part A, Venezia, Italy, 2000*, edited by P. Vincenzini and V. Buscaglia (Techna Srl, Faenza, 2000).
- [50] M. Tinkham, *Introduction to Superconductivity* (McGraw-Hill, New York, 1996).
- [51] T. Nishizaki and N. Kobayashi, Vortex-matter phase diagram in $\text{YBa}_2\text{Cu}_3\text{O}_y$, *Supercond Sci Technol* **13**, 1 (2000).
- [52] E. Zeldov, D. Majer, M. Konczykowski, V. B. Geshkenbein, V. M. Vinokur, and H. Shtrikman, Thermodynamic observation of first-order vortex-lattice melting transition in $\text{Bi}_2\text{Sr}_2\text{CaCu}_2\text{O}_8$, *Nature* **375**, 373 (1995).
- [53] K. Kadowaki and K. Kimura, Precise magnetization measurements of single crystalline $\text{Bi}_2\text{Sr}_2\text{CaCu}_2\text{O}_{8+\delta}$, *Phys Rev B* **57**, 11674 (1998).
- [54] R. H. Koch, V. Foglietti, W. J. Gallagher, G. Koren, A. Gupta, and M. P. A. Fisher, Experimental Evidence for Vortex-Glass Superconductivity in Y-Ba-Cu-O, *Phys. Rev. Lett.* **63**, 1511 (1989).
- [55] M. Suzuki, Y. Yamada, E. Tajitsu, and S. Kojima, Self-Heating in Small Mesa Structures Made of Intrinsic Josephson Junctions in BSCCO, *IEEE Trans. Appl. Supercond.* **17**, 594 (2007).
- [56] Y. Saito, Y. M. Itahashi, T. Nojima, and Y. Iwasa, Dynamical vortex phase diagram of two-dimensional superconductivity in gated MoS_2 , *Phys. Rev. Mater.* **4**, 074003 (2020).
- [57] A. Weber and L. Kramer, Dissipative States in a Current-Carrying Superconducting Film, *J. Low Temp. Phys.* **84**, 289 (1991).
- [58] R. Ikeda, T. Ohmi, and T. Tsuneto, Theory of Broad Resistive Transition in High Temperature Superconductors under Magnetic Field, *J. Phys. Soc. Jpn.* **60**, 1051 (1991).
- [59] A. Yu, T. Zhang, D. Fan, P. Yuan, W. Peng, H. Li, C. Lin, G. Mu, X. Zhang, L. You, Vortex glass phase transition in two dimensional $\text{Bi}_2\text{Sr}_2\text{Ca}_2\text{Cu}_3\text{O}_{10+\delta}$ sub-microbridge, *Supercond. Sci. Technol.* **36**, 035008 (2023).
- [60] for example, S. Ochiai, H. Okuda, M. Fujimoto, J.-K. Shin, M. Sugano, M. Hojo, K. Osamura, S. S. Oh, and D. W. Ha, Analysis of the correlation between n -value and critical cur-

- rent in bent multifilamentary Bi2223 composite tape based on a damage evolution model, *Supercond. Sci. Technol.* **25**, 054016 (2012).
- [61] A. P. Mackenzie, S. R. Julian, G. G. Lonzarich, A. Carrington, S. D. Hughes, R. S. Liu, and D. C. Sinclair, Resistive Upper Critical Field of $Tl_2Ba_2CuO_6$ at Low Temperatures and High Magnetic Fields, *Phys. Rev. Lett.* **71**, 1238 (1993).
- [62] L. Li, J. G. Checkelsky, S. Komiya, Y. Ando, and N. P. Ong, Low-temperature vortex liquid in $La_{2-x}Sr_xCuO_4$, *Nature Physics* **3**, 311 (2007).
- [63] Y.-T. Hsu, M. Hartstein, A. J. Davies, A. J. Hickey, M. K. Chan, J. Porras, T. Loew, S. V. Taylor, H. Liu, A. G. Eaton, M. L. Tacon, H. Zuo, J. Wang, Z. Zhu, G. G. Lonzarich, B. Keimer, N. Harrison, and S. E. Sebastian, Unconventional quantum vortex matter state hosts quantum oscillations in the underdoped high-temperature cuprate superconductors, *Proc. Natl. Acad. Sci. U.S.A.* **118**, 2021216118 (2021).